

Supporting information

Smart off–on copper sulfide photoacoustic imaging agent based on amorphous–crystalline transition for cancer imaging

1. Materials

Copper chloride dihydrate ($\text{CuCl}_2 \cdot 2\text{H}_2\text{O}$) and thioacetamide were purchased from Sigma-Aldrich. Bovine serum albumin (BSA) was obtained from Amersco (Solon, OH, USA). All reagents were used without further purification. The procedures used for mouse selection, care, welfare, and sacrifice were approved by the Animal Ethics Committee of Shanghai Normal University and were in strict accordance with the policy of the Institutional Animal Care and Use Committee.

2. Synthesis of CuS

To prepare the amorphous CuS, 0.2 g of BSA was first dissolved in 40 mL of deionized water and 0.1 mmol of solid copper chloride was then added with stirring. After the formation of a light blue solution, 0.2 mmol of thioacetamide was added and the resulting mixture was incubated at 25 °C in a water bath for 2 h. The amorphous CuS was obtained by centrifugal ultrafiltration with a molecular weight cutoff of 100 kDa and washed three times with water. The crystalline CuS was prepared by incubating the aqueous dispersion of amorphous CuS at 37 °C in a water bath for 48 h.

3. Characterization

The sizes, morphologies, and microstructures of the CuS were analyzed by transmission electron microscopy (TEM; JEM-2010F). X-ray diffraction (XRD) was performed using a Rigaku DMAX 2000 diffractometer equipped with a Cu $K\alpha$ radiation source at a scanning rate of 10°/min in the 2 θ range of 20–80°. UV–visible absorption spectra were acquired on a Shimadzu UV-2550 ultraviolet–visible–near-infrared spectrophotometer using quartz cuvettes with an optical path length of 1 cm. The solution concentration of CuS was determined using high-dispersion inductively coupled plasma atomic emission spectroscopy (ICP-AES; Leeman Labs Prodigy). Fourier-transform infrared (FT-IR) spectra were measured on a Nicolet Avatar 370 FT-IR spectrophotometer using potassium bromide pressed pellets. Hydration size was determined using a Malvern Zetasizer Nano ZS.

4. Photothermal performance tests

To investigate the photothermal performance of the CuS nanoparticles, the temperature changes of aqueous mixtures of CuS with different concentrations (pure water, 10, 25, 50, or 100 $\mu\text{g}/\text{mL}$) were measured using an FLIR A300 thermal camera during irradiation with an 808 nm laser (1 W/cm^2) for 15 min. For the photostability

tests, aqueous mixtures of crystalline CuS (50 $\mu\text{g}/\text{mL}$) were subjected to five cycles of laser irradiation (15 min on and 15 min off).

5. Photoacoustic imaging using CuS

The PA signal was measured by multispectral photoacoustic tomography (MSOT inVision 128, iThera Medical, Germany). The CuS was mixed with 3% agarose, which served as a tissue-mimicking phantom to mimic tissue scattering. After solidification of the agarose, the PA imaging of the CuS was investigated under different conditions.

6. *In vivo* PA studies

The *in vivo* PA images were obtained by multispectral photoacoustic tomography (MSOT inVision 128, iThera Medical, Germany). Pathogen-free five- to six-week-old BALB/c nude mice were purchased from Shanghai SLAC Laboratory Animal Co., Ltd. 4T1 cells (1×10^6) were subcutaneously injected into the flanks of the animals to generate tumors. After the mammary carcinoma (4T1) tumors had reached a diameter of approximately 1 cm, PA images of the tumor-bearing nude mice were taken to serve as the control. Then, a dispersion of amorphous CuS in phosphate-buffered saline (20 μL , 23 mM) was administered by intratumoral injection and PA images were acquired 6, 12, and 24 hours after injection.

7. Figures

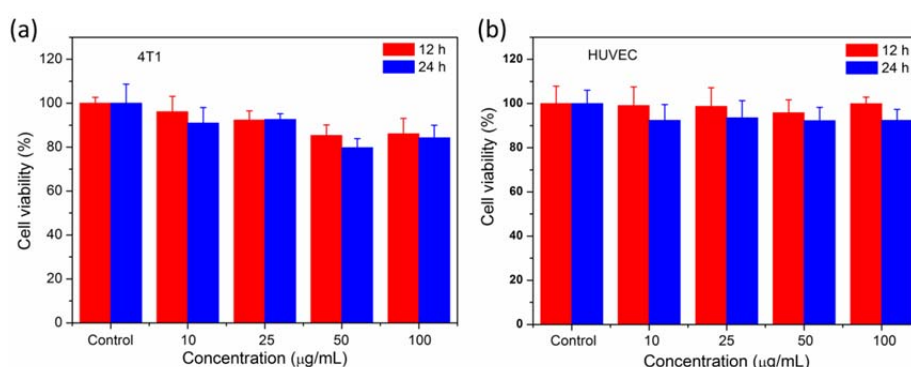


Fig. S1 Cell viability of (a) 4T1 cells and (b) human umbilical vein endothelial cells (HUVEC) after incubation with various concentrations of crystalline CuS (0, 10, 25, 50, and 100 $\mu\text{g}/\text{mL}$) for 12 and 24 h. For both cell types, the cell viability was greater than 80% after incubation with crystalline CuS for 12 and 24 h, demonstrating that the prepared CuS exhibits very good biocompatibility.

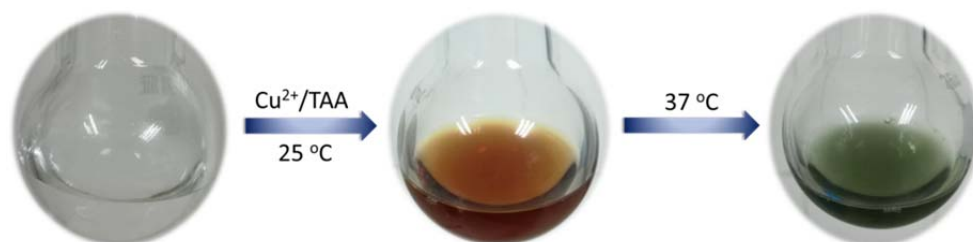


Fig. S2 Temperature-induced color changes during the synthesis of the CuS nanoparticles.

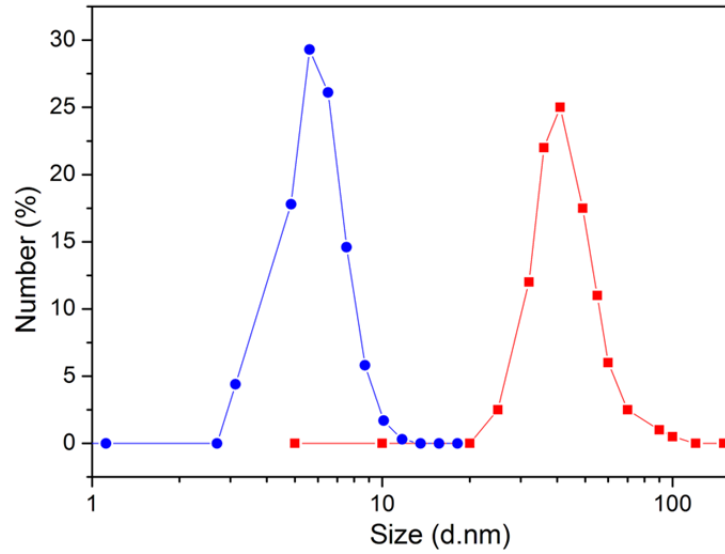


Fig. S3 Hydrodynamic size of the obtained amorphous (blue) and crystalline (red) CuS nanoparticles.

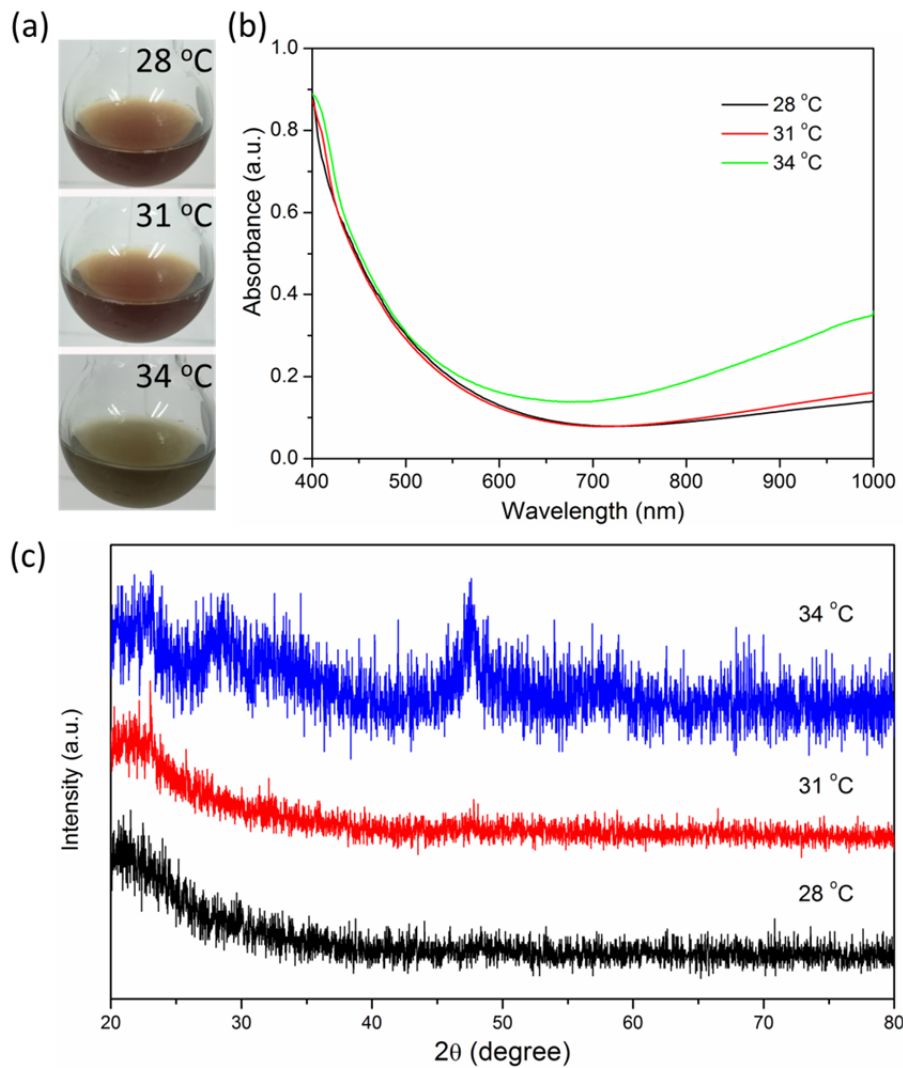


Figure S4 (a) photograph, (b) UV-VIS-NIR absorption spectrum and (c) XRD of the obtained amorphous treated at 28, 31, and 34 °C for 48 h.

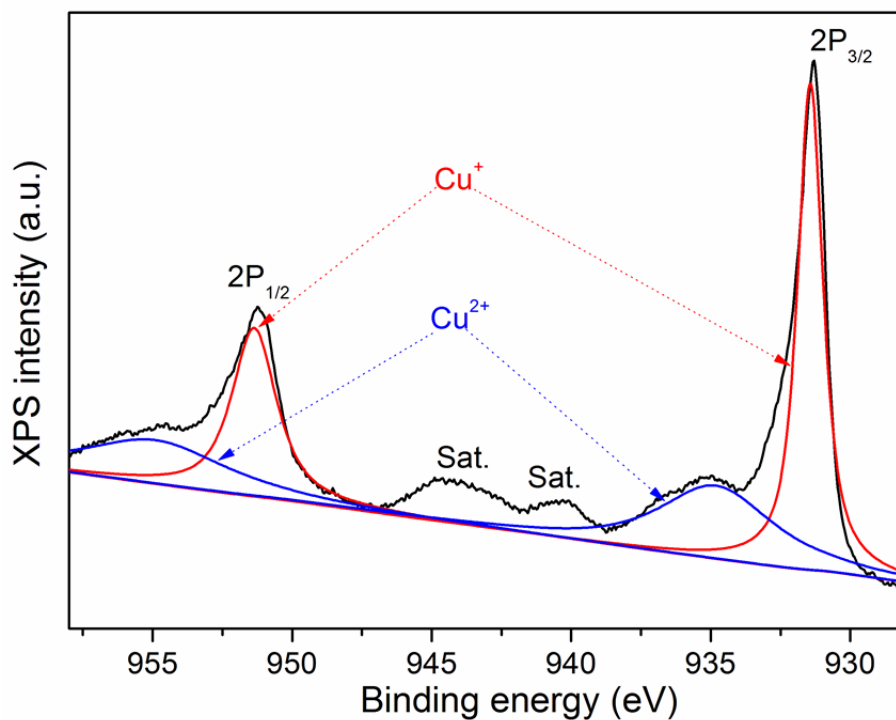


Fig. S5 High-resolution XPS spectra of crystalline CuS in the Cu 2p binding energy region. XPS was used to analyze the electronic state of the CuS after activation. The two intense peaks at 931.4 and 951.4 eV in the high-resolution XPS spectrum of activated CuS are consistent with Cu^+ $2p_{3/2}$ and $2p_{1/2}$, while the satellite (Sat.) peaks and the peaks at 934.7 and 954.5 eV are assigned to the Cu^{2+} oxidation state (Mou, et al. *Biomaterials*, 2015, **57**, 12e21). These results demonstrate the presence of both Cu^{2+} and Cu^+ in the activated CuS nanoparticles.

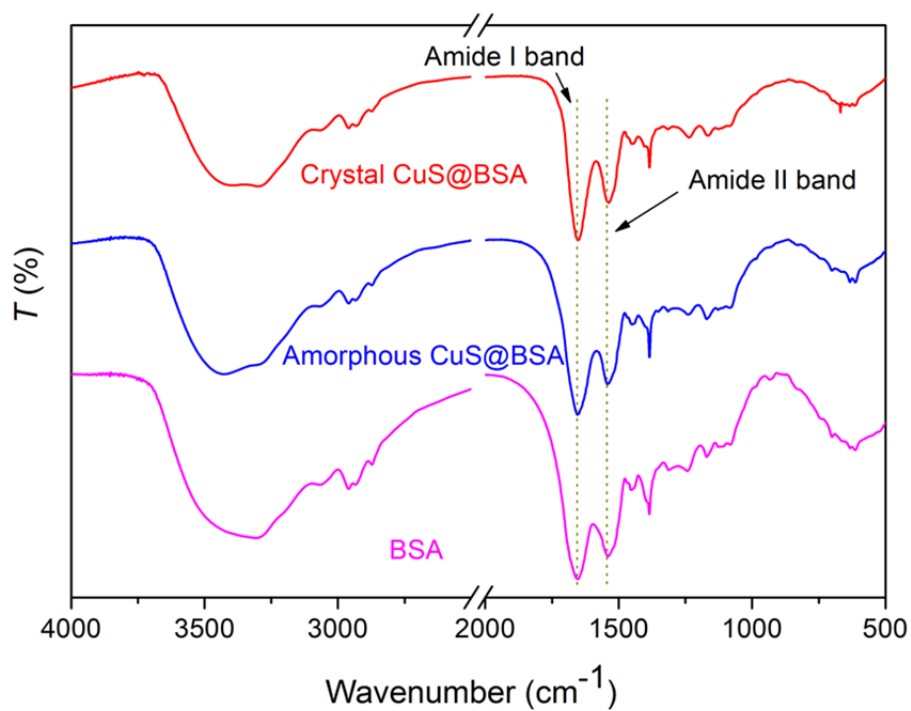


Fig. S6 FT-IR spectra of BSA (magenta) and the obtained amorphous (blue) and crystalline (red) samples of CuS.

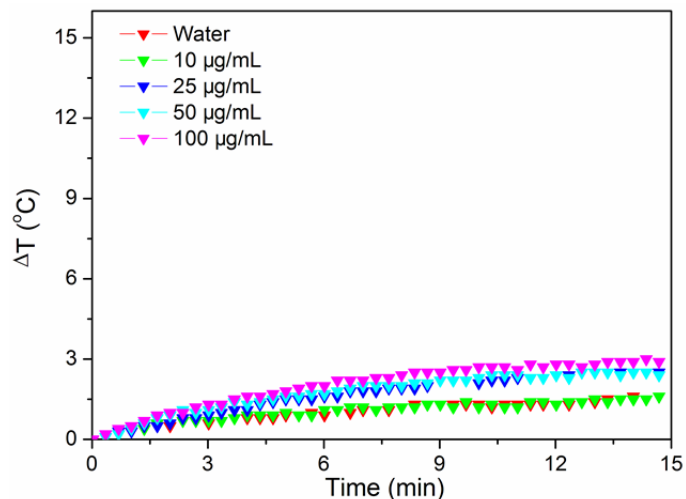


Fig. S7 Temperature increment of amorphous CuS at various concentrations upon irradiation with an 808 nm laser with a power density of 1 W/cm².

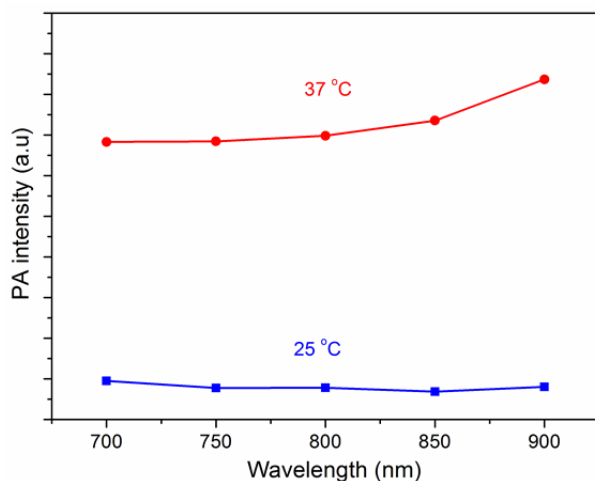


Fig. S8 Photoacoustic spectra of amorphous (blue, 25 °C) and crystalline (red, 37 °C) CuS.

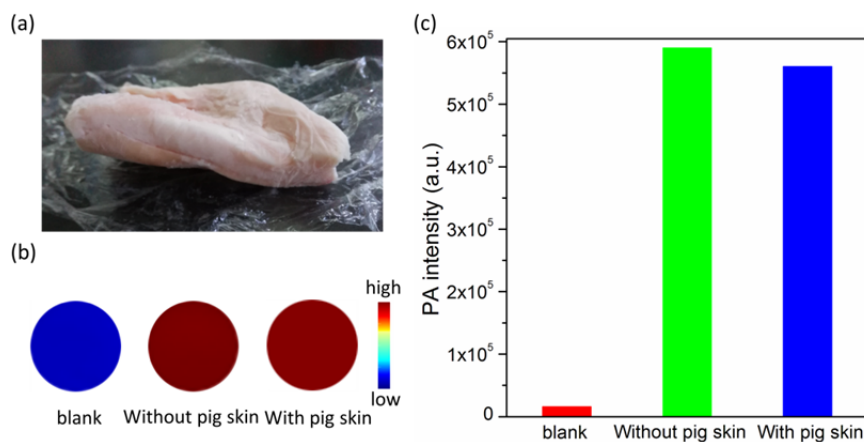


Fig. S9 (a) Photograph of the aqueous dispersion of crystalline CuS after coating with pig skin. (b) PA imaging and (c) corresponding relative signal values of the aqueous dispersion of crystalline CuS with or without the pig skin coating.

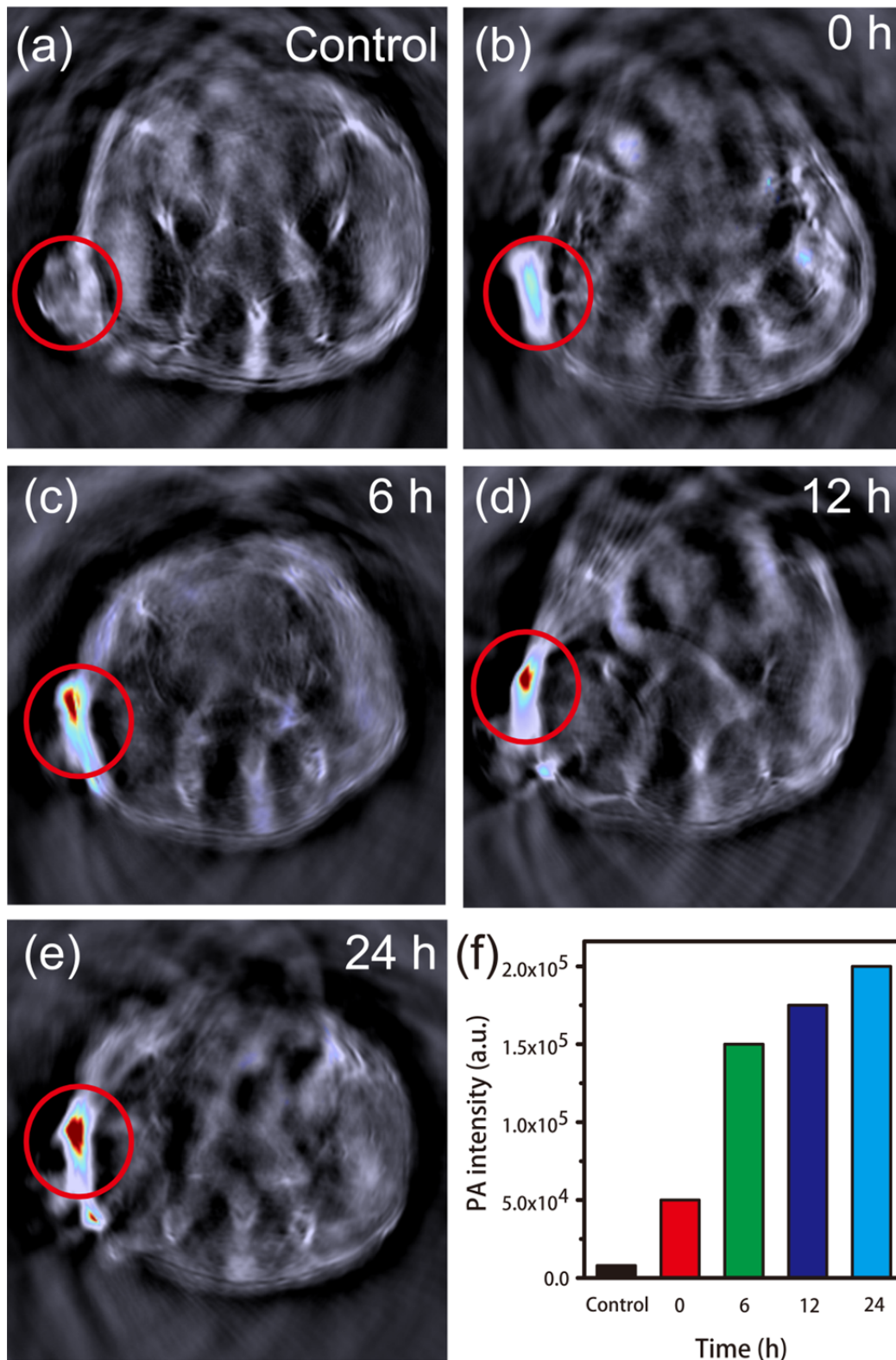


Figure S10 *In vivo* PA imaging obtained at various time points after intratumoral injection of amorphous CuS (20 μ L, 2208 μ g/mL) in tumor-bearing mice (a-e) and corresponding relative signal values (f).

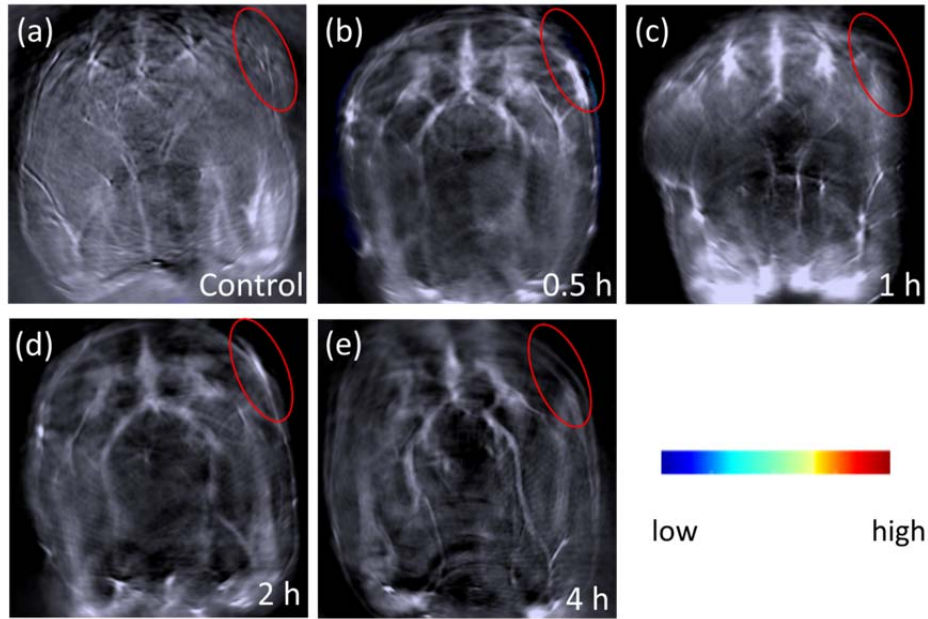


Figure S11 In vivo PA imaging obtained at various time points after intravenous injection of amorphous CuS (20 μ L, 2208 μ g/mL) in tumor-bearing mice. The PA images contrast shows no obviously change at 0.5, 1, 2 and 4h for tumor site compared with control group, indicating that the ultra-small amorphous CuS was removed from the body fast and only little amount of amorphous CuS will accumulate at tumor site.

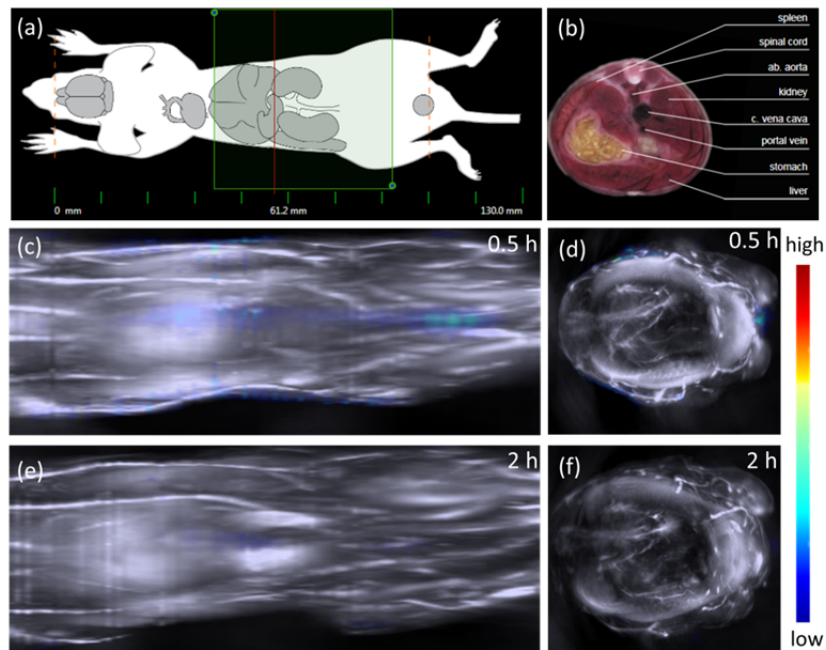


Figure S12 In vivo 3D PA imaging obtained at 0.5 and 2 h after intravenous injection of amorphous CuS (20 μ L, 2208 μ g/mL) in tumor-bearing mice. (a,b) Scheme of the mice for the scan site at sagittal and coronal planes; The sagittal and coronal planes for the 3D PA imaging obtained at 0.5 h (c,d) and 2h (e,f) respectively. The lower contrast differences between 0.5 and 2 h at all the tissue indicate that the diffusion of the CuS nanoparticles and metabolism process will not affect the amorphous-crystalline transition of CuS nanoparticles.

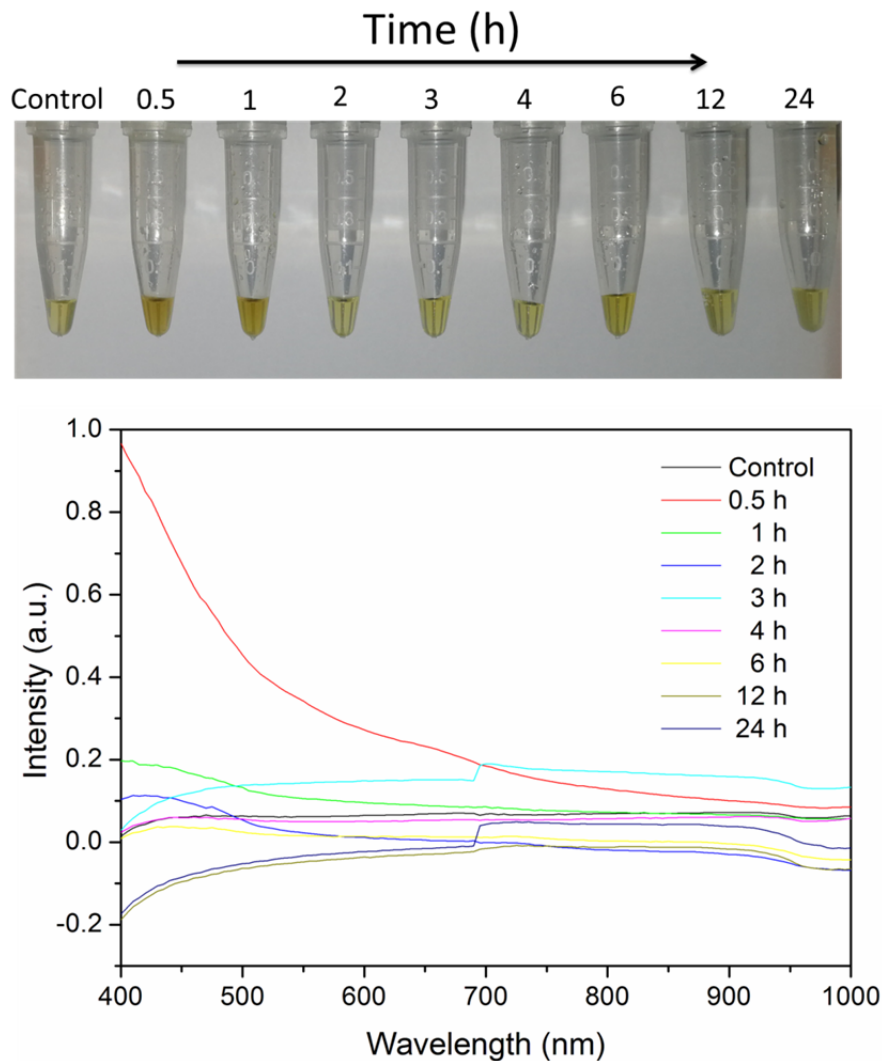


Figure S13 The photograph and UV-VIS-NIR absorption spectrum of the urine for the mice without (control) and with intravenous injection of amorphous CuS (20 μ L, 2208 μ g/mL) at 0.5, 1, 2, 3, 4, 6, 12 and 24 h. The color and absorption the urine after 0.5 h intravenous injection of amorphous CuS is similar with the amorphous CuS, indicating that the ultra-small amorphous CuS was removed from the body fast and the diffusion of the CuS nanoparticles and metabolism process will not affect the amorphous-crystalline transition of CuS nanoparticles.